

Electronic Supplementary Information

Thickness effect on ferroelectric properties of La-doped HfO₂ epitaxial films down to 4.5 nm

Tingfeng Song,^a Romain Bachelet,^b Guillaume Saint-Girons,^b Nico Dix,^a Ignasi Fina,^{*a} and Florencio Sánchez^{*a}

^a Institut de Ciència de Materials de Barcelona (ICMAB-CSIC), Campus UAB, Bellaterra 08193, Barcelona, Spain

^b Univ. Lyon, Ecole Centrale de Lyon, INSA Lyon, Université Claude Bernard Lyon 1, CPE Lyon, CNRS, Institut des Nanotechnologies de Lyon - INL, UMR5270, 69134 Ecully, France.

* ifina@icmab.es, fsanchez@icmab.es

S1: XRD 2θ - χ maps and θ - 2θ scans of films on Si(001)

XRD 2θ - χ frames of the La:HfO₂ films on Si(001) (Figure S1a) show bright circular spots corresponding to the position of STO, the LSMO electrode, and the o-(111) reflection of La:HfO₂. La:HfO₂ m-{002} reflections are detected in the films thicker than 9.2 nm and m-(-111) peak can be observed only in the thickest film. Instead to be circular, the spot is elongated along χ direction. XRD θ - 2θ scans measured with point detector are shown in Figure S1b.

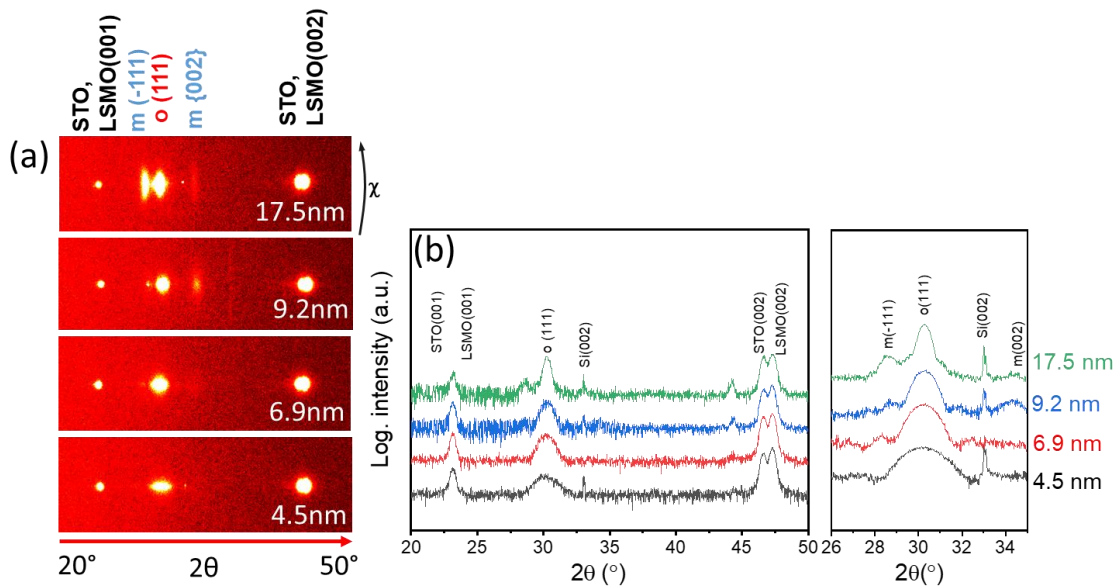


Figure S1. (a) XRD 2θ - χ frames of La:HfO₂ films on Si(001). The χ range is from -10° to 10° . (b) XRD θ - 2θ scans. Right panel: measurement with longer acquisition time around the main La:HfO₂ reflections.

S2: XRD reciprocal space maps

Reciprocal space maps (RSM) around asymmetric $\text{HfO}_2(331)$ and $\text{HfO}_2(402)$ of the $t = 4.5, 6.9$ and 9.2 nm films on $\text{STO}(001)$ were measured (Figure S2). The $\text{HfO}_2(331)$ reflections are close to the (113) reflections of STO and LSMO (here LSMO is indexed as pseudocubic). The $\text{HfO}_2(402)$ reflection is close to the $\text{LSMO}(1.5\ 1.5\ 2.5)$ reflection (there is not an equivalent reflection for STO due to its cubic symmetry). The Q_z axis in both RSM correspond to the $\text{HfO}_2[111]$ direction, whereas the Q_x axis in $\text{HfO}_2(331)$ and $\text{HfO}_2(402)$ corresponds to $\text{HfO}_2[11-2]$ and $\text{HfO}_2[1-10]$ directions, respectively. The out of plane $d_{[111]}$ parameter and the in-plane $d_{[11-2]}$ and $d_{[1-10]}$ parameters of the films, determined from the RSM, are indicated in Table S2-1.

The $d_{[111]}$ parameters are in good agreement with the values determined more accurately from XRD symmetric scans (Figure 1c): 2.977 ($t = 9.2$ nm film), 2.987 Å ($t = 6.9$ nm film) and 2.998 Å ($t = 4.5$ nm film). The in-plane parameters along the $[11-2]\text{HfO}_2(111)$ and $[1-10]\text{HfO}_2(111)$ directions are around 2.11 Å and 3.58 Å, respectively, without significant dependence on thickness. The corresponding values estimated from the calculated lattice constants for bulk orthorhombic HfO_2 ($\text{Pca}21$)¹ are around 2.08 Å and 3.61 Å, respectively. The experimental values determined in our La:HfO_2 films are thus close to the calculated values of relaxed undoped HfO_2 . The relaxed crystal lattice, even in ultra-thin epitaxial La:HfO_2 films, is indeed expected considering that HfO_2 films grow epitaxially on $\text{LSMO/STO}(001)$ by domain matching epitaxy mechanism.²

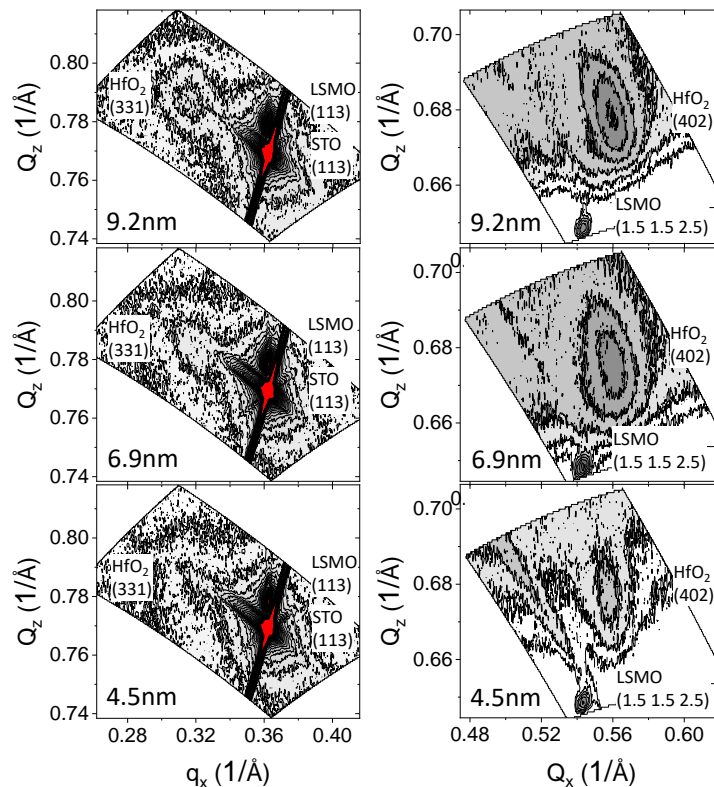


Figure S2: XRD reciprocal space maps around $\text{HfO}_2(331)$ and $\text{HfO}_2(402)$ reflections of La:HfO_2 films of thickness (indicated in the bottom left of each panel) $4.5, 6.9$ and 9.2 nm.

Table S2-1: out of plane $d_{[111]}$ and in-plane $d_{[11-2]}$ and $d_{[1-10]}$ parameters, determined from the RSM around $\text{HfO}_2(331)$ and $\text{HfO}_2(402)$ reflections, of the $t = 4.5, 6.9$ and 9.2 nm films on $\text{STO}(001)$.

Thickness	$\text{HfO}_2(331)$ reflection		$\text{HfO}_2(402)$ reflection	
	$d_{[111]}$	$d_{[11-2]}$	$d_{[111]}$	$d_{[1-10]}$
9.2 nm	2.97 Å	2.11 Å	2.96 Å	3.58 Å
6.9 nm	2.97 Å	2.11 Å	2.97 Å	3.58 Å
4.5 nm	-	-	2.96 Å	3.59 Å

S3: The wake-up effect of films on STO substrate under lower voltage

Figure S3 shows current-voltage curves and polarization-voltage loops in pristine state and after 10 cycles of the films on $\text{STO}(001)$. The maximum applied voltage in each sample is smaller than that applied in Figure 4, and it can be observed that the wake-up effect is more pronounced.

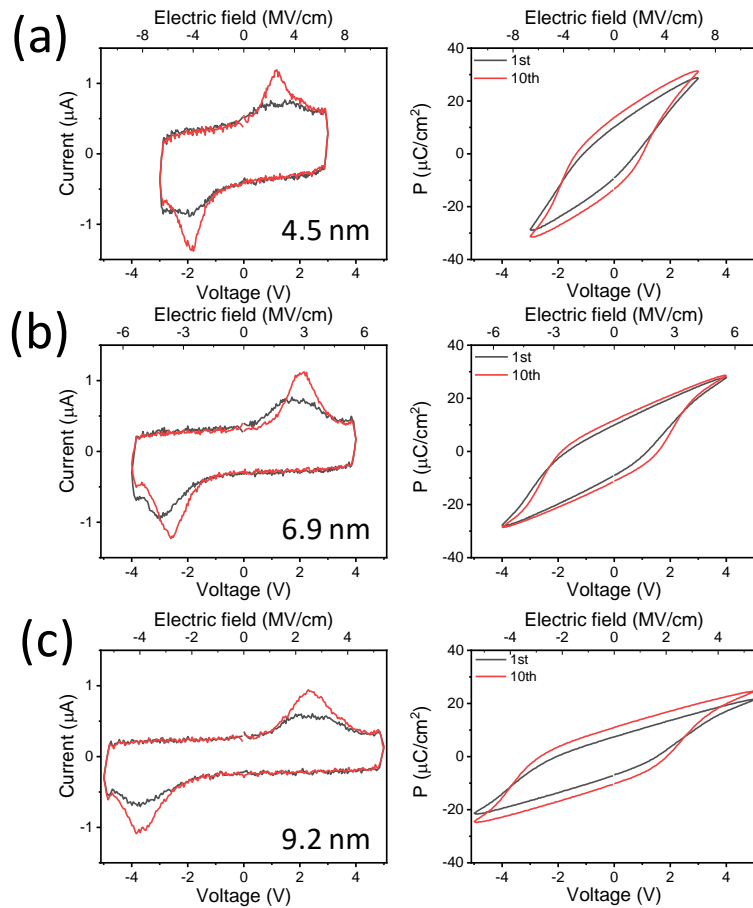


Figure S3. Current-voltage curves and polarization-voltage loops in pristine state and after 10 cycles of La:HfO_2 films on $\text{STO}(001)$ of thickness (a) 4.5 nm, (b) 6.9 nm, (c) 9.2 nm.

S4: The wake-up effect of films on Si(001)

The current-voltage curves and polarization-voltage loops in pristine state and after a few cycles of films on Si(001) are shown in Figure S4. The clear multiple switching current peaks prove the wake-up effect in the 4.5 and 9.2 nm film. The wake-up effect is small and limited to the first cycle.

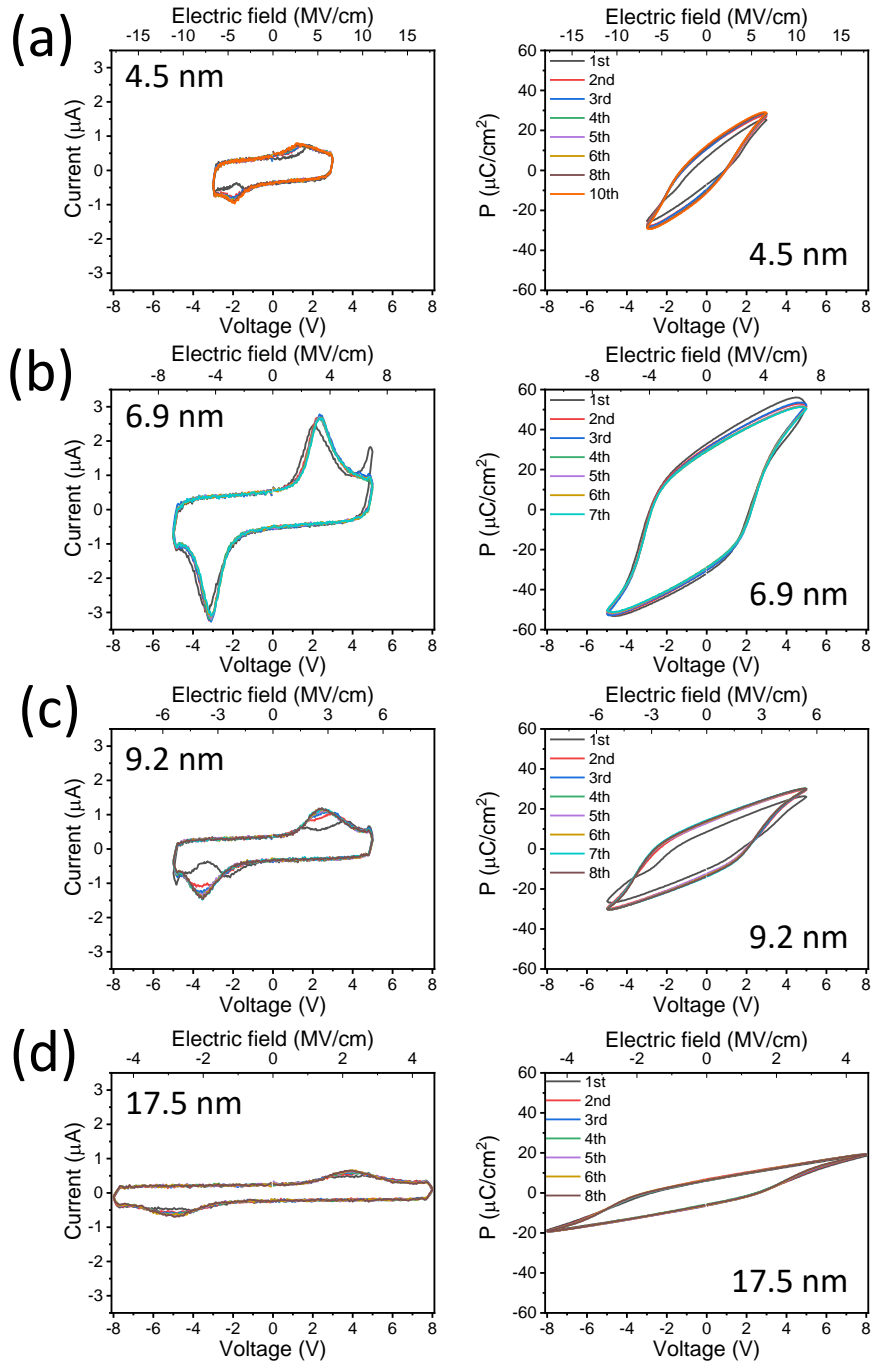


Figure S4. Evolution with the number of cycles of current - voltage curves and the corresponding polarization loops of La:HfO₂ films on Si(001) of thickness (a) 4.5 nm, (b) 6.9 nm, (c) 9.2 nm, and (d) 17.5 nm.

S5: The leakage current of the films on Si(001)

Figure S5a shows leakage current curves of the films on Si(001). The leakage current is in the range from 1×10^{-6} A/cm² to 1×10^{-4} A/cm² at 2 MV/cm. The highest leakage current is in the 4.5 nm film and the 17.5 nm film shows the lowest leakage current. The dependences of the leakage current at 1 MV/cm and 2 MV/cm are presented in Figures S5b and S5c, respectively, for films on STO(001) (solid symbols) and Si(001) (empty symbols). It is evidenced that i) films on Si(001) are more leaky than films on STO(001) and ii) leakage does not decrease monotonically with increasing thickness as the $t = 6.9$ nm films show low leakage. It is evident that leakage is expected to increase when thickness is reduced, but on the other hand, the relative amount of monoclinic phase increases with thickness, and the incoherent grain boundaries between monoclinic and orthorhombic phases are known to be current paths.³ The combination of both factors affecting leakage cause the local minimum at a thickness of around 7 nm in the leakage - thickness graphs.

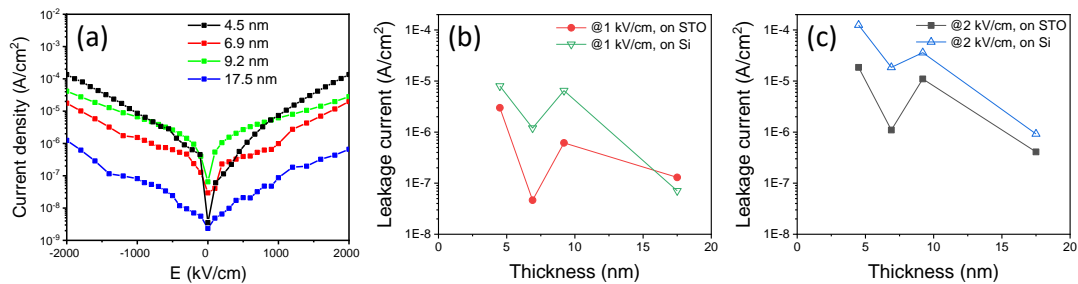


Figure S5. Leakage current curves of La:HfO₂ films on Si(001) (a). Dependence of the leakage current at 1 MV/cm (a) and 2 MV/cm (b) for films on STO(001) (solid symbols) and Si(001) (empty symbols).

S6: The polarization loops after different cycling

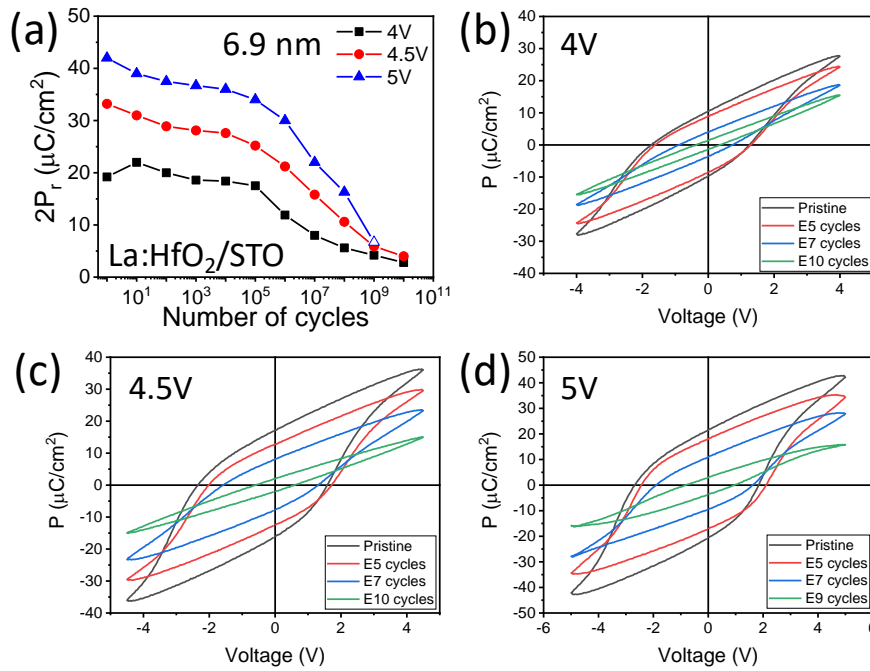


Figure S6. (a) Endurance measurements of the $t = 6.9$ nm La:HfO₂ film on STO(001). polarization loops after a number of bipolar cycles of amplitude 4V (b), 4.5 V (c) and 5 V (d).

S7: Normalized polarization of $t = 6.9$ nm film on STO(001) as a function of the number of cycles

Figure S7 shows the endurance of $t = 6.9$ nm La:HfO₂ film on STO(001) for applied bipolar pulses of different amplitude. Each endurance measurement is plotted with the remanent polarization normalized to the corresponding maximum P_r . It can be seen that the decreasing rate of P_r is very similar under each poling voltage (4 V, 4.5 V, 5 V). Thus, the amplitude of the electric field has nearly no impact on the fatigue. However, the higher voltage promotes breakdown.

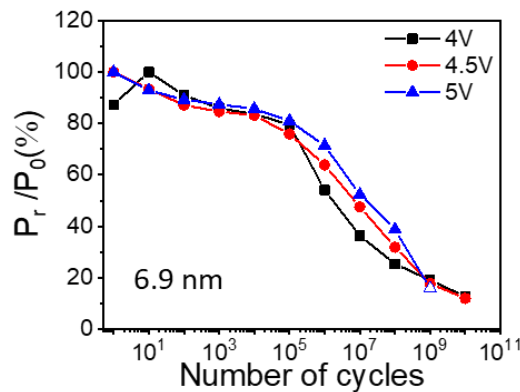


Figure S7. Endurance of the $t = 6.9$ nm film after different cycling. The data after cycling are normalized to the maximum P_r under each voltage. Open symbol indicates breakdown.

S8: Endurance measurement under different cycling frequency

The La:HfO₂ films on STO(001) were measured under different frequency. With frequency increase, fatigue is reduced and endurance is longer.

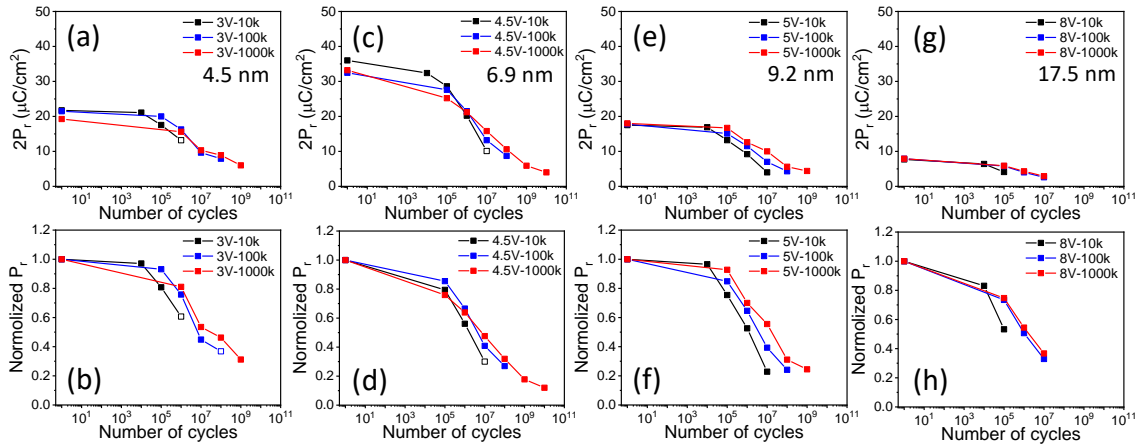


Figure S8. Memory window and normalized polarization of La:HfO₂ on STO(001) films as a function of the number of cycles. Capacitors were cycled at a frequency of 10k (black squares), 100k (blue squares) and 1000k (red squares). The film thickness is (a-b) 4.5 nm, (c-d) 6.9 nm, (e-f) 9.2 nm, (g-h) 17.5 nm. The polarization values are normalized to the maximum P_r under each frequency. Open symbols indicate breakdown.

S9: Endurance and retention of 6.9 nm film on Si(001)

The wake-up effect of the 6.9 nm film on Si(001) is small and limited to a very few cycles, with P_r increasing from 32.4 to 34.1 $\mu\text{C}/\text{cm}^2$. Then, the P_r gradually decrease with cycling, being $2P_r = 5.2 \mu\text{C}/\text{cm}^2$ after 5×10^9 cycles without breakdown. The film also exhibits excellent retention after being poling with the same electric field used to determine the endurance.

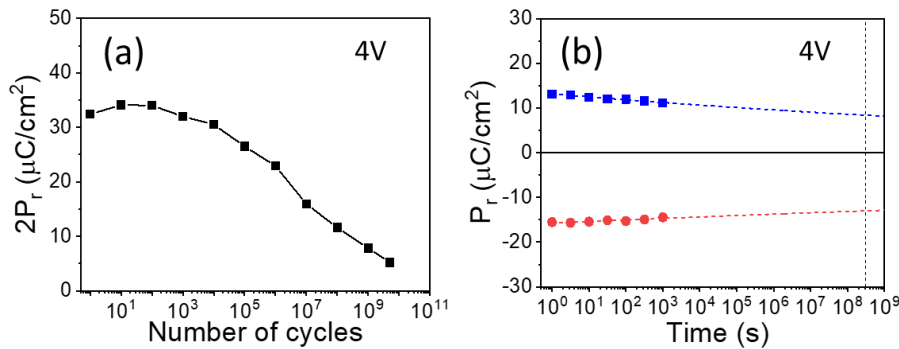


Figure S9. Endurance (a) and (b) retention of the La:HfO₂ 6.9 nm film on Si(001).

References

- 1 L. L. Tao, T. R. Paudel, A. A. Kovalev and E. Y. Tsymbal, *Phys. Rev. B*, 2017, **95**, 1.
- 2 S. Estandía, N. Dix, M. F. Chisholm, I. Fina and F. Sánchez, *Cryst. Growth Des.*,

2020, **20**, 3801.

- 3 M. C. Sulzbach, S. Estandía, X. Long, J. Lyu, N. Dix, J. Gàzquez, M. F. Chisholm, F. Sánchez, I. Fina and J. Fontcuberta, *Adv. Electron. Mater.*, 2020, **6**, 1900852.